



University of Warwick institutional repository: <http://go.warwick.ac.uk/wrap>

This paper is made available online in accordance with publisher policies. Please scroll down to view the document itself. Please refer to the repository record for this item and our policy information available from the repository home page for further information.

To see the final version of this paper please visit the publisher's website. Access to the published version may require a subscription.

Author(s): I. Atkinsona, I. Teoreanu, O.C. Mocioiu, M.E. Smith, M. Zaharescu

Article Title: Structure property relations in multicomponent oxide systems with additions of TiO₂ and ZrO₂ for glaze applications

Year of publication: 2010

Link to published article:

<http://dx.doi.org/10.1016/j.jnoncrysol.2010.04.054>

Publisher statement: "NOTICE: this is the author's version of a work that was accepted for publication in Journal of Non-Crystalline Solids. Changes resulting from the publishing process, such as peer review, editing, corrections, structural formatting, and other quality control mechanisms may not be reflected in this document. Changes may have been made to this work since it was submitted for publication. A definitive version was subsequently published in Journal of Non-Crystalline Solids, [VOL356, ISSUE44-49, October2010, DOI: 10.1016/j.jnoncrysol.2010.04.054"]

Structure property relations in multicomponent oxide systems with additions of TiO₂ and ZrO₂ for glaze applications

I. Atkinson^{1,3}, I. Teoreanu², O.C. Mocioiu¹, M.E. Smith³ and M. Zaharescu¹

1. Institute of Physical Chemistry of the Romanian Academy Bucharest,
202 Splaiul Independentei, 060021 Bucharest Romania

2. University "Politehnica" Bucharest, 1 Polizu Street, District 1, Bucharest, Romania

3. University of Warwick, Physics Department, Coventry, CV4 7AL, UK

Abstract

The influence of the additives (10 weight% rutile, anatase and zirconia) on the atomic scale structure and microstructure of a base glaze (60 wt% feldspar, 15 wt% quartz, 8 wt% kaolin, 12 wt% dolomite and 5 wt% zinc oxide) are investigated. The morphology and structure of the glazes were determined by Scanning Electron Microscopy, X-ray diffraction, infra-red spectroscopy, as well as ²⁷Al and ²⁹Si magic angle spinning (MAS) NMR. Microscopy and X-ray diffraction revealed that the opacity was caused by crystals formed during thermal treatment. Although there are clearly crystalline phases present NMR shows that the heat treated glazes are dominated by the glassy component meaning the opacity is largely conveyed by the added oxide. The relationship between composition, structure and thermal expansion coefficient of the glazes is examined.

1. Introduction

There is significant use of glazes on ceramic products with nowadays a drive to develop glaze compositions that produce an acceptable quality product, but at lower cost. Ceramic glazes are obtained from a variety of raw materials. These include clay minerals, alkaline earth oxides (from carbonate precursors) together with feldspars (which function as source of alkali oxides), alumina and silica [1]. Materials such as ZrO₂, TiO₂, SnO₂ and ZrSiO₄, which give opacity to the glaze, can also be present [2-5]. Understanding and predicting the properties and behavior of glazes, and the effect of additives can be aided by a knowledge of the atomic-scale structure of such materials. Glazes are chemically complex and it is important to have a better understanding of the relationship of compositional parameters, structure and properties in order to satisfy both aesthetical (gloss, transparency or opacity and color) and technical requirements (compatibility with the clay ceramic substrate, with the firing schedule, chemical resistance and good mechanical properties) [6,7]. Many of the glaze properties such as viscosity, thermal expansion coefficient, optical and mechanical are intimately related to the glaze composition since the overall structure results from the contribution and interaction of each component oxide.

Discussion of oxide glass structure relies heavily upon the principle that most cations can be described as either network formers (e.g. Si, B) or network modifiers (e.g.

Ca, Na, K, etc.). Network formers are four-coordinated and bonded to oxygen (e.g. Si–O bonds). The framework and rigidity of such glasses is provided by oxygens that are bonded to two network formers (e.g. Si–O–Si) which are called bridging oxygens (BO). Network modifier oxides break apart this structure through the formation of non-bridging oxygens (NBO), which are bonded to only one network former leaving network modifiers to balance the remaining valence charge of the NBO [7]. Although by definition, silicate glasses contain no long-range order, varying degrees of order may be present locally. This short- to intermediate-range order has been observed directly by magic angle spinning (MAS) nuclear magnetic resonance (NMR), vibration spectroscopy as well as X-ray diffraction.

Here opaque glazes are studied which are those with sufficiently low light transmittance that they effectively hide the ceramic substrate from view [8]. The factors that control the opacity in glazes include the refractive index difference between the glass and opacifier, the number, size, shape and distribution of the opacifier particles, incident light wavelength and glaze thickness. The high refractive indices for TiO₂ (rutile – 2.76 and anatase – 2.52) and ZrO₂ (2.20) compared to that of typical glaze materials (1.50–1.55) make them a good choice for potentially inducing opacity of glazes. TiO₂ addition to ceramic glazes also improves their acid resistance and decreases their viscosity [9]. Monoclinic zirconia (baddeleyite) might be used in complex ceramic glaze formulations as a nucleating agent, with the aim to promote zircon devitrification, which confers opacity and/or an improvement of mechanical properties [5].

The purpose of the work here is to understand how the effect of additions (10 wt%) of rutile, anatase and zirconia, influence the structure and microstructure of a base oxide glaze. Previous studies [10,11] have shown that higher content of opacity additives leads to better aesthetic glaze properties. Since the opacity of glazes is obtained by crystallization of the glass system, SEM studies were additionally performed in order to evaluate the crystals and microstructure formed during the thermal treatment. This study looks at the crystal formation and local structure of the glazes for different additives. The structural characteristics determined are compared to dilatometry results. This information should provide a basis for improving such glazes for ceramic products.

2. Experimental

2.1. Preparation of glazes

A standard raw ceramic glaze with the base chemical composition (expressed in weight%) 60 wt% feldspar, 15 wt% quartz, 8 wt% kaolin, 12 wt% dolomite and 5 wt% zinc oxide) [10] had in separate samples 10 wt% of three opacifiers TiO₂ (rutile and anatase) and ZrO₂ (baddeleyite) added. The overall oxide composition of the individual glazes expressed in molar % including the additive is presented in Table 1. The glazes were synthesized by a traditional ceramic method. The raw materials in the correct proportions were wet milled up to 0.1% residue using a 63 μm sieve. The material:balls:water ratio was 1:1.5:0.6. The slurry obtained was deposited on the green ceramic substrate and thermally treated in an electrical furnace at a maximum temperature of 1250 °C, where it was held for 1 h and then cooled with the furnace.

Table 1 Oxide composition of the prepared glazes (% molar)

Sample	Na ₂ O	K ₂ O	Al ₂ O ₃	ZnO	CaO	MgO	SiO ₂	TiO ₂ rutile	TiO ₂ anatase	ZrO ₂
G0	3.66	3.46	9.43	3.97	8.02	8.02	63.44	-	-	-
G1	3.40	3.21	8.64	3.66	7.33	7.33	58.25	8.18	-	-
G2	3.40	3.21	8.64	3.66	7.33	7.33	58.25	-	8.18	-
G3	3.50	3.30	8.89	3.77	7.55	7.55	59.98	-	-	5.46

2.2. Methods of characterization

X-ray diffraction studies were performed on the powdered samples using Cu K α X-ray radiation, $\lambda = 1.5406 \text{ \AA}$, in the 2θ range of $10\text{--}90^\circ$, on a PANalytical diffractometer. The X-ray tube was operated at 40 kV and 30 mA. The microstructure of the glazes was inspected using a Zeiss SUPRA 55VP Scanning Electron Microscope equipped with energy dispersive analysis of X-ray (EDAX) capability. Infrared transmission spectra were carried out using the same weight of the glaze powder dispersed in KBr pellets. The data were recorded by Nicolet 6700 spectrophotometer $400\text{--}1400 \text{ cm}^{-1}$ domain.

The ^{29}Si magic angle spinning (MAS) NMR spectra were recorded using a Varian InfinityPlus spectrometer with a 7.05 Tesla (T) magnet at a Larmor frequency of 59.6 MHz. The powder samples were packed into 7 mm zirconia rotors and spun at 4 kHz. All the spectra were externally referenced to tetramethylsilane at 0 ppm. The data acquisition conditions were a pulse width of $1.5 \mu\text{s}$ (corresponding to a tip angle of $\sim 30^\circ$), a pulse delay of 20 s, which produced relaxed spectra, with 800 scans co-added.

^{27}Al MAS NMR spectra were recorded using a Bruker Advance II⁺ spectrometer equipped with a 14.1 T magnet (156.37 MHz for ^{27}Al). For the experiment the samples were packed into 3.2 mm zirconia rotors and spun at 18 kHz. $\text{Y}_3\text{Al}_5\text{O}_{12}$ (YAG) was used as reference with the AlO_6 resonance set to 0.7 ppm. The data acquisition conditions were a pulse width of $0.7 \mu\text{s}$ (corresponding to a tip angle of $\sim 15^\circ$), a pulse delay of 1 s with 1800 scans co-added.

The thermal expansion coefficient (α) of the glazes was measured in a quartz dilatometer up to $1000 \text{ }^\circ\text{C}$, at a heating rate of $2 \text{ }^\circ\text{C}/\text{min}$.

3. Results

3.1. Structural characterization

3.1.1. X-Ray Diffraction

Prior to scanning electron microscopy (SEM) studies, X-ray diffraction (XRD) was used for the qualitative determination of the crystalline phases present in the glazes. In figure 1 the XRD patterns of the studied glazes are presented. Examination of the peaks leads to the conclusion that the crystalline phases present in the standard glaze (G0)

are quartz, plagioclase and with some broad underlying intensity indicating residual glassy phase. The plagioclase series ranges from albite to anorthite (with respective composition $\text{NaAlSi}_3\text{O}_8$ to $\text{CaAl}_2\text{Si}_2\text{O}_8$), where sodium and calcium can substitute for each other in this structure. In both glazes with 10% rutile and anatase, rutile was additionally identified in the glaze. In the glaze opacified with baddeleyite, ZrO_2 could be identified besides plagioclase, quartz and zircon.

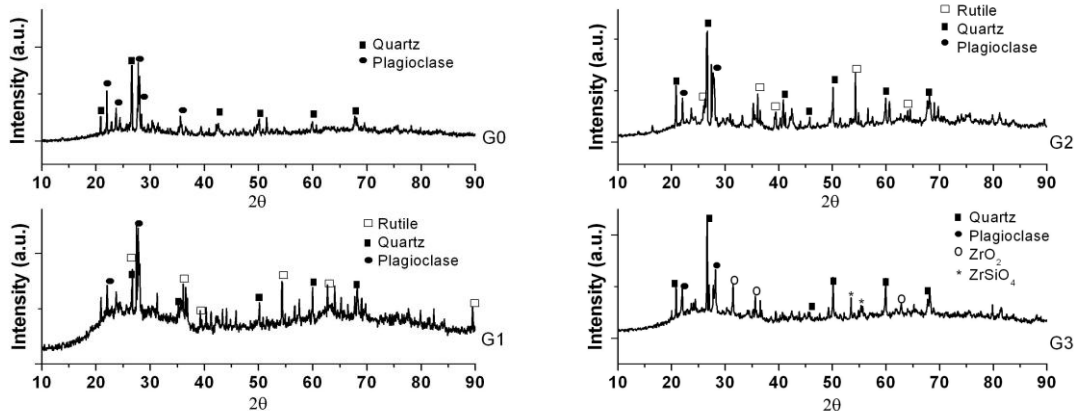


Fig. 1 XRD patterns of the studied glazes

3.1.2 Scanning Electron Microscopy

SEM examination of the glaze-ceramic substrate interfaces shows very good ceramic substrate-glaze adherence. Also, crystalline phases at the glaze-ceramic substrate interfaces can be distinguished. SEM corroborated the XRD indication of different phases present, indicating that the opacity of glazes is due to the presence of different crystalline phases. In the figures 2-4 the micrographs of glaze-ceramic substrate interfaces are presented. In fig. 3(b) EDAX analysis of the interfacial layer for G2 with 10% TiO_2 anatase is also presented.

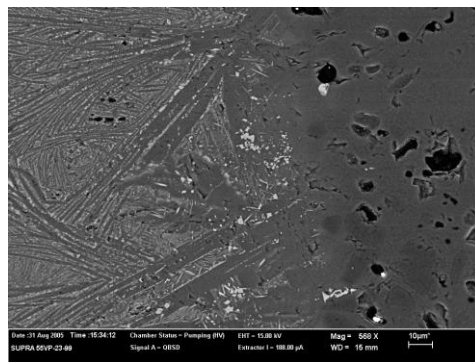


Fig. 2 SEM micrograph of the glaze-ceramic substrate interface for G1 glaze.

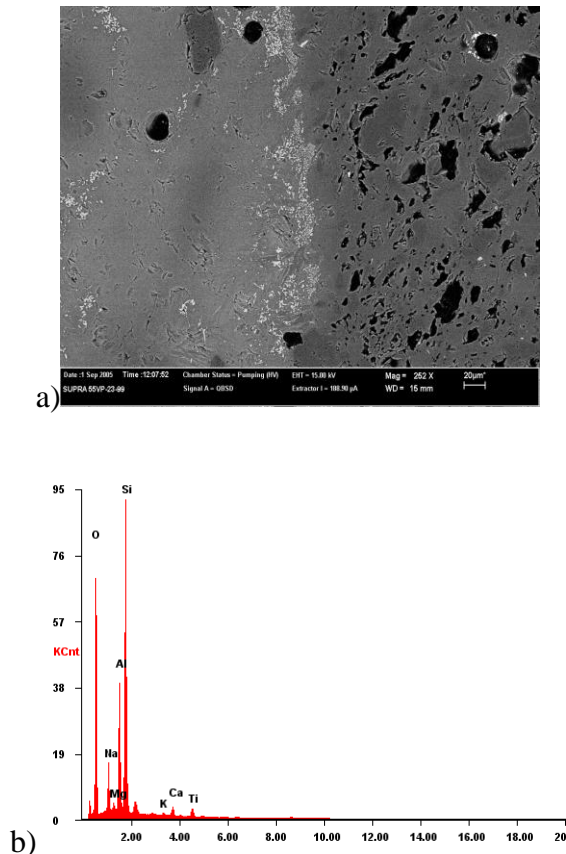


Fig. 3 a) SEM micrograph of the glaze-ceramic substrate interface for G2 glaze and b) EDAX result of the interface analysis

The interface for the glazes with 10% TiO_2 (rutile and anatase) exhibits acicular crystals of rutile embedded in the glassy phase. EDAX analysis of the glaze-ceramic substrate interface shows a higher Si and Al content and lower quantity of Ti.

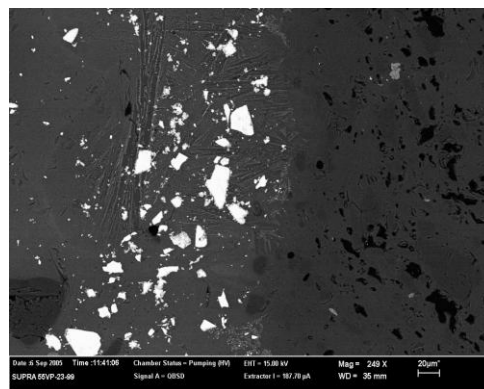


Fig. 4 SEM micrograph of the glaze-ceramic substrate interface for G3 glaze

The interface for G3 glaze shows the presence of ZrO_2 (prismatic crystals) and acicular crystals that could be assigned to ZrSiO_4 .

3.1.3. Infra-Red Spectroscopy

In figure 5 IR spectra of the studied glazes are presented which show broad bands due to overlapping effects of vibration and rotation of structural groups which are characteristic of solids in the vitreous state. Various authors have reported infrared spectra of alkali silicate, aluminosilicate, and alkali aluminosilicate glasses and tried to interpret the observed bands in relation to the glass structure. The general agreement is that all these silicate glasses exhibit at least three bands in the 1100 cm^{-1} , 800 cm^{-1} and 500 cm^{-1} regions, and in some cases another weak band appears at about 950 cm^{-1} [12].

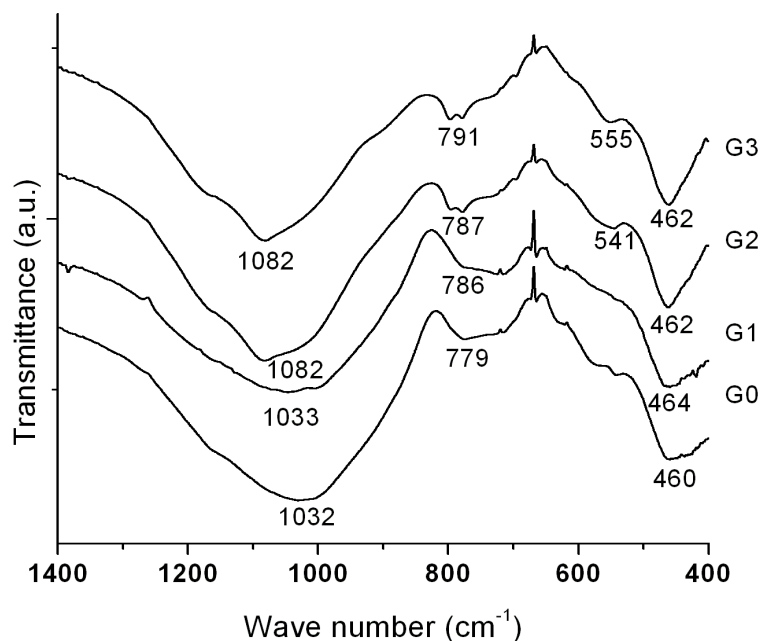


Fig. 5 IR spectra of the studied glazes

In all spectra, the broad bands at 1032 cm^{-1} for G0 and G1 glazes and at 1082 cm^{-1} for G2 and G3 glazes are assigned to Si-O stretching motion in SiO_4 units. The 1100 cm^{-1} band reported for pure silica shifts to a lower frequency as aluminum is introduced in place of silica. There are no sharp peaks in the present glazes, and all the bands are quite broad. From this observation it may be said that the glazes studied here exhibit a somewhat disordered structure [12]. At around 790 cm^{-1} , the characteristic symmetric Si-O-Si stretching vibrations of SiO_4 units are observed [12]. The band at 460 cm^{-1} is assigned to asymmetric deformation vibrations (δ) of SiO_4 units [13].

In the case of the addition of the opacifiers supplementary vibration bands have been observed. In the case of ZrO_2 addition, based on the literature data indicates the 574 and 732 cm^{-1} bands as being characteristic of the monoclinic phase of zirconia [14], the band at 555 cm^{-1} could be ascribed to this component in these samples [15]. The band of the monoclinic zirconia phase that occurs at 732 cm^{-1} overlaps the symmetric Si-O-Si stretching vibrations of the SiO_4 units.

In the FT-IR spectra, the presence of the TiO_2 rutile phase identified by XRD, could be assigned for the G2 glaze, to the low intensity peak at 540 cm^{-1} and for the glaze

G1 to the shoulder that appear in the same region. The peak is assigned to TiO_6 units according to the literature data [16].

3.1.4. ^{29}Si MAS NMR

^{29}Si MAS NMR spectroscopy provides direct information about the structure of materials from measurements of the isotropic chemical shift. The chemical shift for SiO_4 units occur in the range -60 to -120 ppm (with respect to TMS). The chemical shift is influenced most significantly by the coordination number of the Si. ^{29}Si NMR spectra are sensitive to changes in local environment and ^{29}Si resonances can yield isotropic chemical shift characteristic of various Q^n structural groups, where Q denotes silicon in four-fold coordination and $n = 0$ to 4 representing the number of these oxygens bridging to other tetrahedra of the network. The silicate monomer Q^0 occurs at the most positive shift, followed in a regular sequence by Q^1 to Q^4 groups shifted by about 10 ppm to higher field for each Si-O-Si bond [17-19]. The second factor that influences the chemical shift is the number and the type of first cation neighbor. The silicon environment in aluminosilicates can be designated as $\text{Q}^n(\text{mAl})$, where n denotes the number of BO for each Q unit and m represents the number of attached AlO_4 ($m \leq n$). The substitution by Al of each of the four silicons surrounding the central Si of a Q^4 group results in a change in the chemical shift of about 5 ppm towards less negative values. As a result five distinct chemical shift ranges for $\text{Q}^4(0\text{Al})$, $\text{Q}^4(1\text{Al})$, $\text{Q}^4(2\text{Al})$, $\text{Q}^4(3\text{Al})$ and $\text{Q}^4(4\text{Al})$ are observed [17,20].

Figure 6 presents ^{29}Si MAS-NMR spectra of the obtained glazes. All the spectra are considerably broader than the base glaze with no opacifier. Very broad lines are observed for highly disordered systems such as amorphous or glassy materials, whereas narrow peaks are obtained for perfectly ordered systems [17]. The key point here is that although XRD shows the presence of crystalline components there are no sharp lines present in the corresponding ^{29}Si MAS NMR spectra. This indicates just how low the content of silicon-containing crystalline phases is in these glazes. The increase in the ^{29}Si peak width of the glasses (glaze) relative to aluminosilicate crystals is probably due to both an increase in the range of aluminium next nearest neighbors of silicon and an increase of the range of bond angles and bond distance for each type of silicon site. Murdoch *et al.* [21] showed that the ^{29}Si NMR line widths of alkali and alkaline-earth aluminosilicate glasses increase as the cation polarization power (Z/r :charge/radius) increases, at fixed Si/Al ratios.

Simulations using one, two and three Gaussian peaks were done for the ^{29}Si NMR spectra using Dmfit software [22]. The positions, widths and amplitudes of the Gaussians were varied in order to obtain the best fit with the minimum number of peaks are summarized in Table 2. The precision and accuracy is about ± 1 ppm for the chemical shift, ± 0.5 kHz for the FWHM and $\pm 2\%$ for the intensity. The ^{29}Si MAS NMR spectrum for the G0 glaze has a maximum at -96 ppm and is well simulated by a single Gaussian peak. The spectrum for glaze G1 has three Gaussian peaks, while two Gaussian peaks are necessary to simulate the spectra from glazes G2 and G3 as can be seen in figure 7.

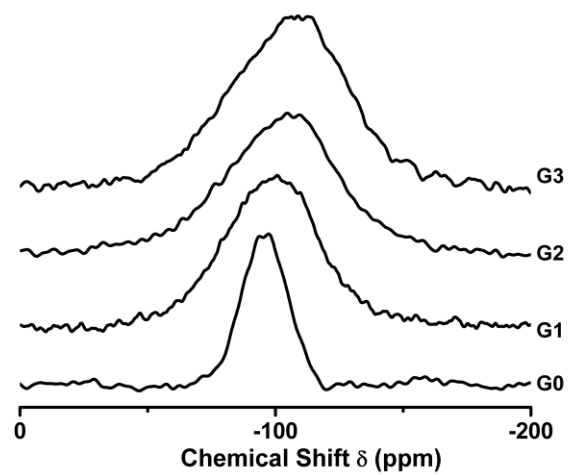


Fig. 6 ^{29}Si MAS NMR spectra of the studied glazes

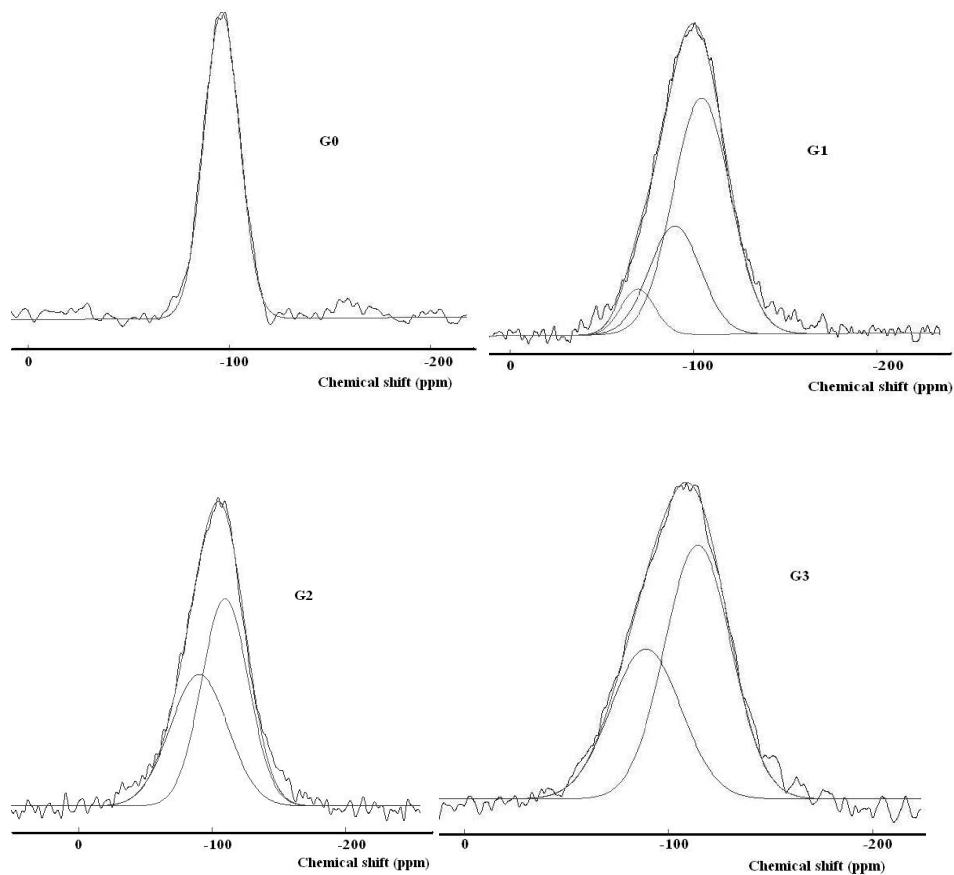


Fig. 7 Deconvoluted ^{29}Si MAS NMR spectra of studied glazes

Table 2 Solid state ^{29}Si MAS NMR data

Sample	Peak 1			Peak 2			Peak 3		
	δ	FWHM	%	δ	FWHM	%	δ	FWHM	%
	(ppm)	kHz		(ppm)	kHz		(ppm)	kHz	
G0	-96	1.2	100	-	-		-	-	-
G1	-104	2.2	65	-90	2.0	27	-70	1.3	8
G2	-110	2.5	56	-90	1.1	44	-	-	-
G3	-114	2.4	61	-89	2.4	39	-	-	-

FWHM-full width at half maximum; δ -chemical shift

Standard glaze G0 gives a chemical shift of -96 ppm which could be assigned to $Q^4(2\text{Al})$ site [23]. Alkali and alkaline earth aluminosilicate glasses generally show peaks that can be assigned to $Q^4(2\text{Al})$ and $Q^4(3\text{Al})$ sites [24]. Chemical shifts of -110 ppm and -114 ppm corresponding to $Q^4(0\text{Al})$ could be assigned to Si in a vitreous silica-like phase. The chemical shift of -104 ppm correspond to $Q^4(1\text{Al})$. The peaks at around -89 to -90 ppm, could be assigned to $Q^4(3\text{Al})$ indicating further ordering of the aluminosilicate network [23]. The peak of -70 ppm for G1 glaze can be assigned to Q^1 .

3.1.5. ^{27}Al MAS NMR

^{27}Al MAS NMR is used for examining the coordination of aluminum atoms in both polycrystalline and amorphous materials, but a detailed quantitative analysis of the spectra is more difficult to due second-order quadrupole effects [17]. The chemical shift for aluminum is around 50-80 ppm for AlO_4 , 10-15 ppm for AlO_6 and 30-40 ppm for AlO_5 , in well crystallized compounds [17]. In aluminosilicates, AlO_4 groups are bonded exclusively to Si tetrahedra (Lowenstein's rule [25]). In glasses, the three chemical shift ranges characteristic of the Al spectrum are obtained only in the case of rapid cooling, while in the case of slower cooling the glasses usually contain only AlO_4 and AlO_6 .

In fig. 8 ^{27}Al MAS NMR spectra of the studied glazes are presented. The ^{27}Al spectral data are given in table 3. The FWHM of ^{27}Al peaks are not reported, because this nucleus experiences second-order quadrupolar peak broadening [26]. The precision and accuracy is about ± 1 ppm for the chemical shift and $\pm 2\%$ for the intensity.

The spectra of G0 and G1 glazes exhibit two peaks, one at around 55 ppm corresponding to AlO_4 and at around 13 ppm corresponding to AlO_6 . The spectra of G2 and G3 glazes consist of a peak at 55 ppm which is assigned to AlO_4 [27]. The broader low intensity peak around 0 ppm in these samples is a spinning sideband.

Al^{3+} ions are glass network intermediates such that they can act as both network formers and network modifiers. When Al^{3+} ions enter as network formers as AlO_4^- , there need to be metal ions (e.g. Me^+ , Me^{2+}) in their vicinity to produce local electrical charge balance [11].

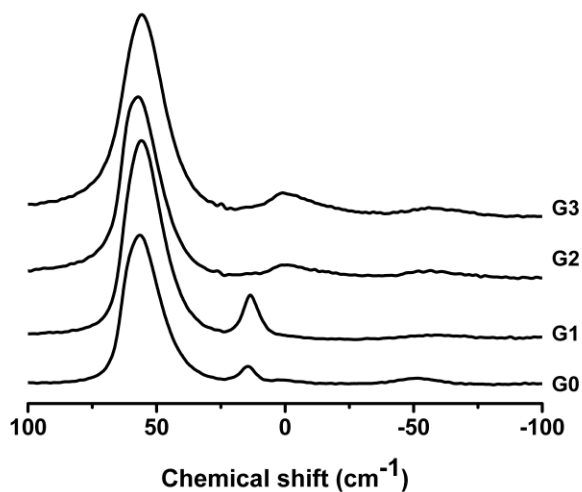


Fig. 8 ^{27}Al MAS NMR spectra of the studied glazes

Table 3 Solid state ^{27}Al MAS NMR data

Sample	Peak 1		Peak 2	
	δ_{peak} ppm	%	δ_{peak} ppm	%
G0	56	95	14	5
G1	56	89	12	11
G2	55	100	-	-
G3	55	100	-	-

3.1.6 Dilatometry results

In order to investigate if there is a relationship between thermal expansion coefficient (α) and the chemical composition of glazes, α was determined experimentally and calculated using the additivity law (Appen method) Eq. (1) [28]. This law assumes that each oxide has a different contribution to the final α value. This contribution is described by an oxide characteristic coefficient (α_i) and, thus, α can be estimated by Eq. (1):

$$\alpha = \frac{1}{100} \sum \alpha_i p_i \cdot 10^{-7} \quad (1)$$

where: α_i is the characteristic parameters of the component oxides and p_i is the fraction of initial oxides expressed in molar fraction. Table 4 indicates the dilatometry results for the studied glazes.

Table 4 Dilatometry results

Sample	$\alpha \cdot 10^{-6}$ ₃₀₀ experimental [1/grd]	$\alpha \cdot 10^{-6}$ calculated [1/grd]
G0	5.37	6.90
G1	5.20	6.51
G2	5.22	6.51
G3	4.73	6.23
$\alpha_{\text{substrate experimental}} = 5.50 \cdot 10^{-6}$ [1/grd]		

It can be observed that the calculated values in Table 4 show some deviations from experimental values since the glazes are not homogeneous (i.e. crystallization occurs). The difference between thermal expansion coefficient of the glazes and thermal expansion coefficient of the ceramic substrate should ideally be less than 15% to allow good adherence during thermal cycling. A difference in expansion coefficient between body and glaze of more than 15% creates stress in the cold glaze [8]. The obtained data indicates that the additives decrease the thermal expansion coefficient values of the glazes compared to that free of additives.

4. Discussion

XRD and SEM comparative studies reveal the presence of supplementary phases besides quartz and plagioclase when the additives are used. In the case of glazes with TiO₂ (anatase and rutile) the presence of rutile was observed, explained by the anatase-rutile transformation during the thermal treatment [9]. From a melt the high temperature stable phase always crystallizes, that is rutile here. In the glaze opacified with baddeleyite (ZrO₂), ZrO₂ could be identified along with plagioclase, quartz and zircon. The presence of the acicular crystals with low dimensions could be assigned to the crystallization of ZrSiO₄ during cooling of the glazes, while the crystals of large size represent ZrO₂ particles that have not melted during the glaze preparation.

For glazed ceramic products the adhesion of the cover layer is of high importance. The adhesion characteristics are formed during the thermal treatment when a reaction between the glaze and the ceramic body takes place. The interaction layers can be formed containing crystals which may or may not be thermally compatible with either body or glaze and they would thus affect the overall strength of the system. The glaze-ceramic interactions depend on the chemical composition of the ceramic substrate and glaze, the thickness of the glaze layer, the thermal treatment and the viscosity of the molten glazes [29]. In the thin layer between the ceramic body and the glaze surface no pores are visible. This interaction layer can influence glaze properties, especially thermal expansion coefficient and the occurrence of defects such as pin-holes and cracks.

FT-IR spectra confirm the results obtained by XRD and SEM, and show that the glazes containing additives have supplementary vibration bands characteristic of zirconia and TiO₆ units. The shift of the main band maximum from 1100 cm⁻¹ to lower frequencies may be related to a decreased degree of polymerization of the SiO₄ groups

[30]. In terms of the effect of composition on the glaze properties it is known that ZrO_2 improves the wear rate of the glazes and TiO_2 decreases the glaze viscosity and improves acid resistance [9,31,32].

^{29}Si MAS NMR results show that the glazes have a tetrahedral framework structure with a wide range of local coordinations $Q^4(0Al)$, $Q^4(1Al)$, $Q^4(2Al)$ and $Q^4(3Al)$ present producing broad spectral lines. The structure of the most silica-rich aluminosilicate glasses ($Si/(Si+Al) = 0.9$), as in the case of the studied glazes, are dominated by $Q^4(0Al)$ and $Q^4(1Al)$ sites [27]. A key observation is despite XRD revealing crystalline plagioclase phases that there are no corresponding ^{29}Si MAS NMR signals. This apparent contradiction is readily explained as XRD strongly favours any crystalline component. ^{29}Si NMR is directly quantitative and shows that the silicate-content of the glaze is effectively all in the glassy phase despite the XRD results. ^{27}Al MAS NMR spectra of G2 and G3 glazes indicate that they have a fully polymerized tetrahedral framework structure. For these glazes, the only ^{27}Al signal detected was for AlO_4 . For G0 and G1 glazes a signal around 15 ppm indicating the presence of AlO_6 was observed probably indicating that some of the aluminum could be charge balancing some of the AlO_4^- .

The influence of the composition and structure of the obtained glazes on their properties was evaluated by dilatometry. Dilatometry results show good glaze-ceramics substrate adherence for all the studied glazes. The thermal expansion of glass is not only a function of temperature, but also depends among other factors such as composition, structure of the glass, e.g., degree of polymerization, type of structural units, the nature and contribution of the different cations and whether they occupy forming or modifying positions in the glass network [33,34]. The crystallization process greatly altered the thermal expansion of the glazes. Therefore, the polycrystalline materials may have high or low coefficients of expansion depending on the expansion coefficient and elastic properties of the crystal phases formed and the residual glass matrix [33].

5. Conclusions

Glazes for sanitary ceramics, opacified with 10% TiO_2 (rutile and anatase) and ZrO_2 , respectively were obtained. The crystallization behavior and microstructural evolution of the glazes showed the development of rutile and zircon crystals as indicated by XRD, SEM and FT-IR within the glassy matrix. The opacity of these glazes is largely due to the presence of the crystals formed which is dominated by the added oxides. IR indicates that the glazes are in general highly disordered. ^{29}Si MAS NMR data clearly shows that on addition of the opacifiers the glaze becomes much more highly disordered and although XRD shows silicon-containing crystalline phases, the silicon is effectively contained within the glassy phase. This indicates that using the complementarity of XRD and NMR is essential so as not to get a misleading impression of the actual distribution between glassy and crystalline components. Aluminum largely acts as a network former in these glazes, with the majority of the aluminum as AlO_4 , but in some samples small amounts of AlO_6 form. The dilatometry results demonstrated good adherence of the studied glazes on the ceramic substrate.

Acknowledgements

I. (Gresoiu) Atkinson gratefully acknowledges the financial support from the European Commission for a Marie Curie scholarship “Solid State NMR of Inorganic Materials” to the University of Warwick, UK. MES thanks EPSRC for partial funding of the NMR facilities at Warwick.

References

- [1] A.P. S. Mandair and W. R. McWhinnie, *Polyhedron*, 9 (1990) 1709.
- [2] E.Bou, A. Moreno, A. Escadrino, A. Gozalbo, *Journal of the European Ceramic Society* 27 (2007) 1791.
- [3] M. Romero, J. Ma. Rincon, A. Acosta, *Journal of the European Ceramic Society* 23 (2003) 1629.
- [4] N. M. Bobkova, L.V. Boloban, S. A. Gailevich, *Glass and Ceramics* 54 (1997) 17
- [5] S. A. El-Defrawi, M. A. Serry, W. I. Abd El-Fattah and W. Weisweiler, *Ceramics International* 21 (1995) 69.
- [6] M. Llusar, G. Monro'sa, C.M. Rodriguesb, J.A. Labrinchac, *Ceramics International* 31 (2005) 181.
- [7] C. I. Merzbacher, B. L. Sherriff, S. J. Hartman, W. B. White, *J. Non-Cryst. Solids* 124 (1990) 194.
- [8] R. A. Eppler, D. R. Eppler, *Glazes and Glass Coatings*, The American Ceramic Society, Ohio, 2000
- [9] S. Teixeira, A. M. Bernardin, *Dyes and Pigments* 80 (2009) 292.
- [10] V. Burghilea, I. Gresoiu, M. I. Popescu, D. Nicolae, *Romanian Journal of Materials* 36 (2006) 171
- [11] I. Atkinson, I. Teoreanu, M. Zaharescu, *Romanian Journal of Materials*, 39 (2009), 202.
- [12] B. N. Roy, *J Am Ceram. Soc.*, 73 [4] (1990) 846.
- [13] A. N. Moreva, I. A. Levitskii, *Glass and Ceramics*, 63 (2006) 122.
- [14] S. K. Saha, P. Pramanik, *J. Non-Cryst. Solids* 159 (1993) 31
- [15] J. Chandradass, K.-S. Han, D. S. Bae, *Journal of Materials Processing Technology* 206 (2008) 315
- [16] M. Crisan, A. Jitianu, M. Zaharescu, F. Mizukami and S. Niwa, *Journal of Dispersion Science and technology*, 24 (2003) 129
- [17] K. J. D. MacKenzie, M. E. Smith. *Multinuclear Solid State NMR of Inorganic Materials*. Pergamon Press, Oxford, 2002
- [18] L. Olivier, X. Yuan, A.N. Cormack, C. Jager, *J. Non-Cryst. Solids*, 293-295, (2001), 53.
- [19] E. Lippmaa, M. Magi, A. Samoson, G. Engelhardt, A.-R. Grimmer. *J. Am. Chem. Soc.* 102 (1980) 4889.
- [20] M. Magi, E. Lippmaa, A. Samoson, G. Engelhardt, A.-R. Grimmer, *J. Phys. Chem.* 88 (1984) 1518.
- [21] J. B. Murdoch, J.F. Stebbins, I. S. E. Carmichael, *Am. Mineral.* 70 (1985) 332.

- [22] D. Massiot, F. Fayon, M. Capron, I. King, S. Le Calvé, B. Alonso, J.-O. Durand, B. Bujoli, Z. Gan, G. Hoatson, *Magn. Reson. Chem.*, 40 (2002) 70.
- [23] A. P. S. Mandaïr, W. R. McWhinnie, *Polyhedron*, 10 (1991) 55.
- [24] G. Engelhardt and D. Michel, *High Resolution Solid NMR of Silicates and Zeolites*, (Wiley, New York, 1987).
- [25] W. Lowenstein, *Am. Mineral.* 39 (1954) 92.
- [26] M. E. Smith, E. R. H. van Eck, *Prog. Nucl. Magn. Reson. Spectrosc.* 34 (1999) 159.
- [27] R. Oestrike, W. H. Yeang, R. J. Kirkpatrick, R. L. Hervig, A. Navrotsky, B. Montez, *Geochimica Cosmochimica Acta*, 51 (1987) 2199.
- [28] M. G. Rasteiro, T. Gassman, R. Santos, E. Antunes, *Ceramics International* 33 (2007) 345.
- [29] A. Kara, R. Stevens, *J. Eur. Ceram. Soc.*, 22 (2002) 1095.
- [30] I. A. Levitskii, *Glass and Ceramics*, 60, (2003), 111
- [31] K.J. Hong, J.M. Kim, H.S. Kim, *J. Eur. Ceram. Soc.*, 23 (2003) 2193.
- [32] W. Heimsoeth and F.R. Meyer, *J. Am. Ceram. Soc.* 34(1951) 366.
- [33] S.N. Salama, E. A. Saad, H. Darwish, H.A. Abo-Mosallam, *Ceramics International* 31 (2005) 559.
- [34] T. Kopar, V. Ducman, *Materials Characterization* 58 (2007) 1133.